http://dx.doi.org/10.5935/0103-5053.20150094

J. Braz. Chem. Soc., Vol. 26, No. 6, 1274-1282, 2015.
Printed in Brazil - ©2015 Sociedade Brasileira de Química
0103 - 5053 $6.00+0.00

Article

Novel and Fast Microwave-Assisted Synthesis of Carbon Quantum Dots from Raw Cashew Gum

*Natalia R. Pires, Clara M. W. Santos, Rayane R. Sousa, Regina C. M. de Paula, Pablyana L. R. Cunha and Judith P. A. Feitosa**

Laboratório de Polímeros, Departamento de Química Orgânica e Inorgânica, Universidade Federal do Ceará, Caixa Postal 6021, 60455-760 Fortaleza-CE, Brazil

Carbon quantum dots (C-dots) with average size of 9 nm were synthesized from an aqueous solution of raw cashew gum (RCG) using a novel and fast microwave-assisted technique which involves two steps. In the first step (partial depolymerization in solution) some monomer units are formed through the autohydrolysis of CG and a small amount of 5-hydroxymethyl furfural can be obtained. The second step involves polycondensation/polymerization to give rise to a polyfuranic structure followed by aromatization/carbonization and nuclear burst. At the end of the process a composite of partially depolymerized CG and C-dot was formed. A mechanism involved in microwave-assisted two-steps synthesis was suggested. Although no passivation reagent was used, an intensely blue photoluminescent material in UV light was obtained. C-dot was characterized by spectroscopy in the medium infrared, thermal analysis, gel permeation chromatography, transmission electron microscopy, zeta potential, and photoluminescence.

Keywords: carbon quantum dots, cashew gum, microwave-assisted synthesis, photoluminescence

Introduction

Carbon quantum dots (C-dots) are a new class of carbon nanomaterials, with sizes of < 10 nm, which were accidently discovered in 2004.[1] They have emerged as an intriguing material due to their high water solubility, bright photoluminescence in the visible spectrum, low toxicity, good biocompatibility, high stability and easy functionalization.[2,3] The unique properties of C-dots lead to promising applications in biosensing, cellular imaging, drug delivery and catalysis. Inspired by the variety of applications, there is a growing interest in the synthesis of new carbon dots. Laser ablation of carbon targets, pyrolysis, electrochemical shocking of carbon nanotubes (CNTs), electrochemical exfoliation of graphite, hydrothermal treatments, plasma treatment, ultrasonic treatment and microwave heating are the synthetic routes that generate C-dots.[2] Hydrothermal treatments based on autoclave and microwave techniques are the main routes employed.[4-17]

The synthesis procedure using an autoclave requires 2.5-12.0 h of hydrothermal heating at temperatures up to 200 °C,[4-10] and in some cases strong alkaline solutions,[4] or organic solvents[6,8] need to be used. When a microwave is employed, the irradiation time decreases significantly (1-10 min).[11-17] In all these cited studies, surface passivation agents were added before the synthesis. An additional and time-consuming step, such as dialysis for one to several days,[11,12,14,15,17] has to be added in order to obtain purified C-dots. This step removes the advantage of microwave based on the low time consumption.

Carbohydrate-based precursors such monosaccharides, polysaccharides and other raw materials are the main carbon source to synthesize low-cost C-dots. Low molar mass carbohydrates, such as glucose,[18,19] and sucrose,[18] and also fructose and maltose,[20] have been described. Chitosan,[9] alginic acid and starch,[16] and peach gum[10] are examples of polymeric carbohydrates applied as a carbon source. Raw material containing carbohydrate, such as bagasse,[4] grape juice,[5] orange juice,[6] sugar cane juice,[8] and plant leaves[21] have also been studied. Low cost and sustainability are important criteria for selecting carbohydrates as a carbon source to produce C-dots.

Herein, a novel microwave-assisted procedure for the synthesis of carbon dots, based on two steps (depolymerization in solution and partial carbonization in a solid) is reported. An abundant and low-cost raw material (an exudate from the cashew nut tree known as cashew gum) is the precursor employed. Cashew gum is

*e-mail: judith@dqoi.ufc.br

a polysaccharide that contains monosaccharide units such as galactose, glucose, arabinose, rhamnose, and glucuronic acid,[22] Ca, K, Mg and Na, and has a low protein content.[23] Cashew trees are abundant in several countries including Brazil, where the potential annual cashew gum production is around 50,000 tons.[24] As an additional advantage, no organic solvents or passivation reagents are required in this procedure.

Experimental

Chemicals

Crude samples of cashew gum were collected from native trees (*Anacardium occidentale*) in Fortaleza, Ceará State, Brazil and used without purification. All aqueous solutions were prepared with distilled water.

Preparation of carbon quantum dots

An aqueous solution of raw gum (0.5% m/v) was filtered and heated in a domestic microwave (800 W, 100% of total power) for 30-40 min using a rotating plate. The solution dried in the first 18-22 min and then in the last minutes partial carbonization occurred with the formation of a light brown solid. After cooling to ambient temperature, the solid was dissolved in water and centrifuged at 25,000 g for 15 min to remove the less luminescent particles. The upper solution was freeze dried and a pale brown solid was obtained. The solid was considered to be a C-dot composite. The composite yield was determined after freeze drying and is reported as the average value for two experiments.

Characterization of carbon dots

Transmission electron microscopy (TEM) was performed on a Carl Zeiss LIBRA120 electron microscope in-column, operating at 120 kV with a thermionic electron emission filament (LaB_6). All images were obtained in energy filtered transmission electron microscopy (EFTEM) mode with filtering at 0 eV. The hydrogen, nitrogen and carbon contents were determined by elemental microanalysis using a Perkin-Elmer CHN 2400 instrument. The particle size distribution was calculated based on 670 particles from different images. The Fourier transform infrared (FTIR) spectra of the raw polymer and C-dot composite were recorded in solid state in KBr pellets using a FTLA 2000 (ABB Bomem) operating between 400 and 4000 cm^{-1}. The peak molar mass (Mpk) was determined by gel permeation chromatography (GPC) with a Shimadzu LC-20AD instrument at room temperature using an PolySep Linear (7.8 × 300 mm), flow rate of 0.5 mL min^{-1}, sample concentration of 0.1% (m/v), water as the solvent and 0.1 mol L^{-1} $NaNO_3$ as the eluent. An RID-10A refractive index and an SPD-20A UV-Vis were used as detectors. The flow rate was 0.5 mL min^{-1}, sample concentration 0.1% (m/v) and sample volume 25 μL. Pullulan samples (Shodex Denko) of average molar mass 5.9×10^3, 1.18×10^4, 4.73×10^4, 2.12×10^5 and 7.88×10^5 g mol^{-1} were used as standards. The standard curve of log Mpk *vs.* elution volume (Ve) gave the equation:

$$\log Mpk = 13.603 - 1.021Ve \quad (1)$$

Thermogravimetric analysis (TGA) of the samples was carried out under synthetic air flow using a Shimadzu TGA-50 instrument at a heating rate of 10 °C min^{-1} over the temperature range of 25-700 °C. The air flow rate was maintained at 60 mL min^{-1} and the initial sample weight was 10 mg. Surface charge analysis via zeta potential measurements of the raw and purified gum and the C-dot composite was carried out by electrophoretic mobility tests on a Malvern Zetasizer Nano ZEN 3600. A Shimadzu UV-1800 spectrometer was used to record the emission spectra. The photoluminescent (PL) measurements of the raw gum and C-dot composite were recorded using a QuantaMaster50 spectrometer (Photon Technology International) employing concentrations of 0.11% (m/v). Photographs of the C-dot composite solution at different λ_{exc} wavelengths were taken through a lateral opening in the spectrometer with a quartz curvet inside the sample holder. The emission spectra were obtained at excitation wavelengths starting at 360 nm with 20 nm increments.

Quantum yield measurements

The photoluminescence quantum yield (Φ) was measured using quinine sulfate in 0.1 mol L^{-1} H_2SO_4 as the standard, with Φ_{QS} equal to 54% and employing the equation:[8]

$$\Phi_{C\text{-}dot} = 100\Phi_{QS}\frac{I_{CDot}}{I_{QS}}\cdot\frac{A_{QS}}{A_{CDot}}\cdot\frac{\eta^2_{C\text{-}dot}}{\eta^2_{QS}} \quad (2)$$

where I_{CDot} and I_{QS} refer to the integrated luminescence intensity (λ_{exc} at 365 nm) of carbon dot composite and quinine sulfate, respectively. The parameters A and η are the absorbance at 365 nm obtained from the UV spectra, and the refractive index of the solvents used, respectively. The subscripts Cdot and QS are related to the same samples as specified for the I parameter. The solution concentrations were adjusted to achieve an absorbance of less than 0.1.

Results and Discussion

Characterization of carbon dots

No detectable photoluminescence was shown by the raw material solution. In daylight the C-dot solutions were light yellow-brownish and in UV light an intense blue emission was observed. The maximum wavelength and the color emitted are dependent on the wavenumber of excitation (Figure 1a). When the excitation wavelength changes from 350 to 650 nm the emission color changes from blue to red and the PL intensity decreases. Similar behavior was reported by Sun *et al.*[25] The absorption spectrum for the C-dots showed a peak centered at 278 nm, which is, in general, attributed to the π-π* transition of C=C bonds and n-π* transition of C=O bonds and shoulders at 369 nm, probably ascribable to aromatic π orbitals[17] (Figure 1b). There was no detectable absorption for the cashew gum.

Figure 2 shows the EFTEM images of the carbon dots, which were mostly spherical with an average diameter of 9 ± 3 nm. Thus, they are larger than the major C-dots reported in the literature (2-5 nm).[4-8,10,12,17,20,21,26] Higher values (7-10 nm) have also been observed.[9,11,16] The presence of a polymeric phase was also detected in C-dot from cashew gum (image not shown), and this indicates that the synthesized material is a composite of C-dots and polysaccharide. In addition to the amorphous carbon material, a lattice spacing of 0.42 nm can be observed (Figure 2b, magnification 315,000×). Values of 0.18-0.23 nm have been attributed to a diamond-like structure,[20,26] [102] facet of graphitic carbon,[5,6] and [100] facet of graphitic carbon.[20,21] A lattice spacing of 0.31-0.34 nm has been assigned to the [002],[19] and [003][20] spacing of graphitic carbon. An interlayer spacing of 0.42 nm has been previously detected in C-dots obtained from orange juice[6] and sucrose,[27] and attributed to poor crystallization.[27]

FTIR spectra were used to identify the functional groups which remained in the C-dot composite (C-dot + polysaccharide) (Figure 3a). The FTIR spectra

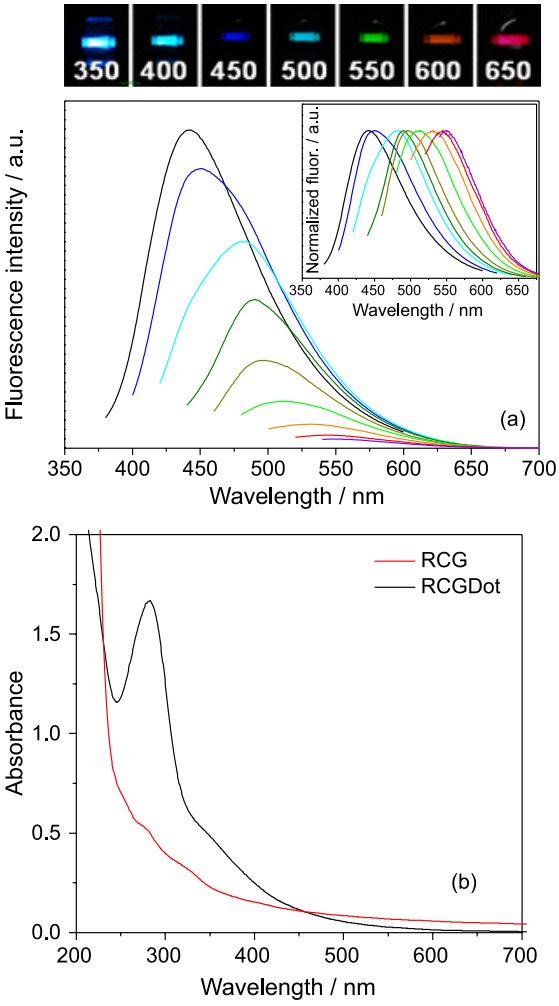

Figure 1. (a) Luminescence emission spectra (unnormalized and normalized) and emitted color for C-dots from raw cashew gum excited at different wavelengths; (b) absorption spectra for aqueous solution of raw cashew gum and C-dot.

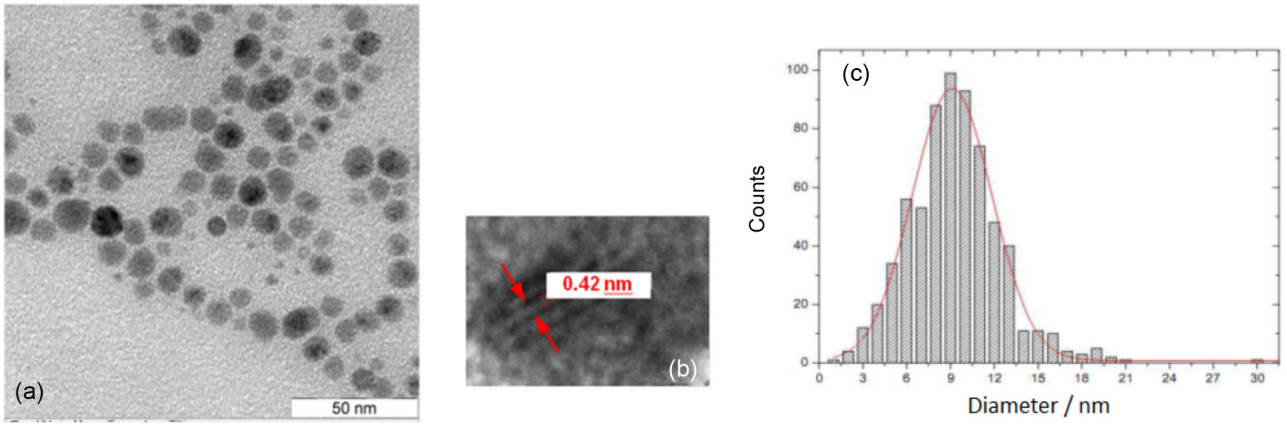

Figure 2. (a) EFTEM image of C-dot from raw cashew gum; (b) enlarged image showing a lattice spacing; (c) particle size distribution. Red line: Gaussian distribution.

for the raw gum showed characteristic bands, such as those at 3412 cm^{-1} (OH stretching vibration), 2926 and 2855 cm^{-1} (symmetric and asymmetric CH stretching), 1423 cm^{-1} (OH bending/COO^- asymmetric stretching) and 1166-1020 cm^{-1} (C–O, C–O–C, and C–C stretching vibrations of the hexopyranosyl). The band at 1648 cm^{-1} could be due to the OH vibration originating from the polysaccharide moisture content and also COO^- symmetric stretching from the salt form of glucuronic acid (4.7-6.3%).[22,24]

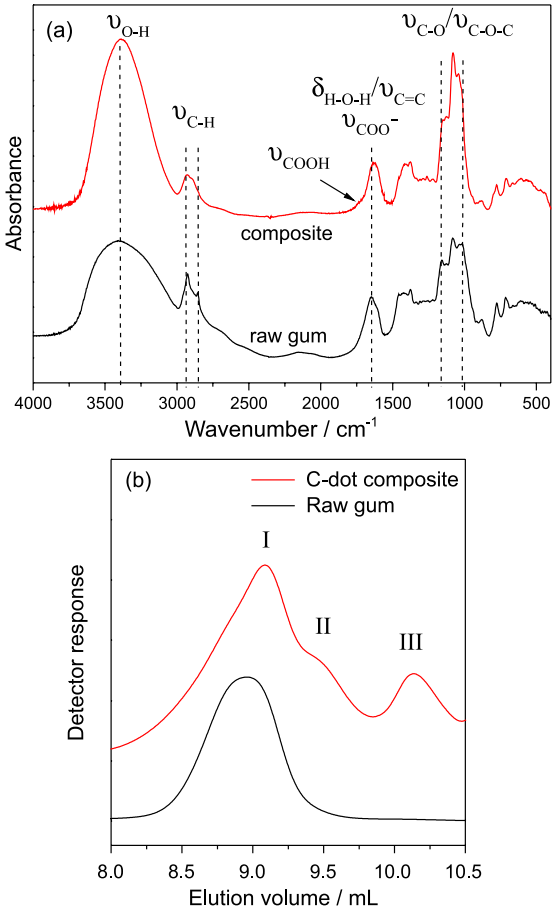

Figure 3. (a) FTIR spectra and (b) GPC curves for raw cashew gum and C-dot composite using refractive index detector.

Slight differences in the spectrum for the composite compared with that for the initial gum can be observed: the proportions of OH and C–O/C–O–C increased (3388 and 1020-1160 cm^{-1}, respectively), the proportion of CH decreased (2900 cm^{-1}) and COOH appears (shoulder at 1733 cm^{-1}). A band shift from 1648 (gum spectrum) to 1628 cm^{-1} (C-dot composite spectrum) suggested the formation of a C=C bond, in the range of 1620-1660 cm^{-1} on the FTIR spectra for other C-dots.[5,8,10,17] The groups observed in the C-dots originating from polysaccharides are the same: O–H, C–O and COOH.[6,16,18] They improve the hydrophilicity and stability in aqueous systems.

Important information on the composition of the C-dot composite can be obtained by GPC. In this technique macromolecules are separated according to their molar mass or hydrodynamic volume. Larger molecules elute first. The curves obtained for the raw gum and composite were very different (Figure 3b). The macromolecules from the raw gum presented a monomodal distribution with a Ve of 8.94 mL while a multimodal distribution with three fractions was observed for the composite. The contributions of each fraction were calculated from the corresponding area as: I (86.1%), II (3.6%), and III (10.3%). The GPC curve for the composite solution using a UV-Vis detector at wavelength of 280 nm (curve not showed) exhibited only peak III, indicating that this fraction contains the C-dot. The main peak I and the shoulder II correspond to the polysaccharide without the C-dot and constituted 89.7% (m/m) of the whole composite. This high content of polysaccharide is in agreement with the slight change in the FTIR spectrum of the composite in comparison with the precursor gum.

The Mpk values, calculated using equation 1, for the polysaccharides in the composite (I: 22,000 g mol^{-1}, II: 7,000 g mol^{-1}) are lower than those for the original gum (30,400 g mol^{-1}), indicating the occurrence of chain degradation in these fractions. Since no increase in the carbon percentage was observed by elemental analysis of the composite, the content of carbon particles in the C-dot is assumed to be small. The nanoparticle is probably comprised of a core of tiny carbon particles decorated with oligo/polysaccharide.[18] The Mpk of fraction III (C-dot) is 1,800 g mol^{-1}. Considering that oligosaccharide molecules surround all of the carbon particles, the oligomeric sugar bonded to them could have an Mpk of 900 g mol^{-1} - a dimension equivalent to five units of monosaccharide. The composite contains 10.3% (m/m) of C-dot and oligosaccharides are attached to the carbon dot surface.

The raw gum and composite thermal decomposition processes show one water loss event (up to 200 °C), and two main events at the temperature of maximum decomposition (Tm) in the ranges of 220-350 and 400-500 °C (Figure 4). The event at around 300 °C is attributed mainly to the loss of CO_2. Depolymerization, decarbonylation and the evolution of products containing O–H, C–H, C=O, C–C and C–O also occur, but to a lesser extent. In the range of 400-500 °C the events are due to the pyrolytic decomposition of carbonaceous material formed during the degradation of the polysaccharide chain.[28] The thermal decomposition of the composite ended first and a greater amount of residue was observed. The oxidative decomposition of graphite begins at 600 °C.[29] The residue at 550 °C (2.0%) may represent the percentage of carbon particles. The final residue for the raw gum

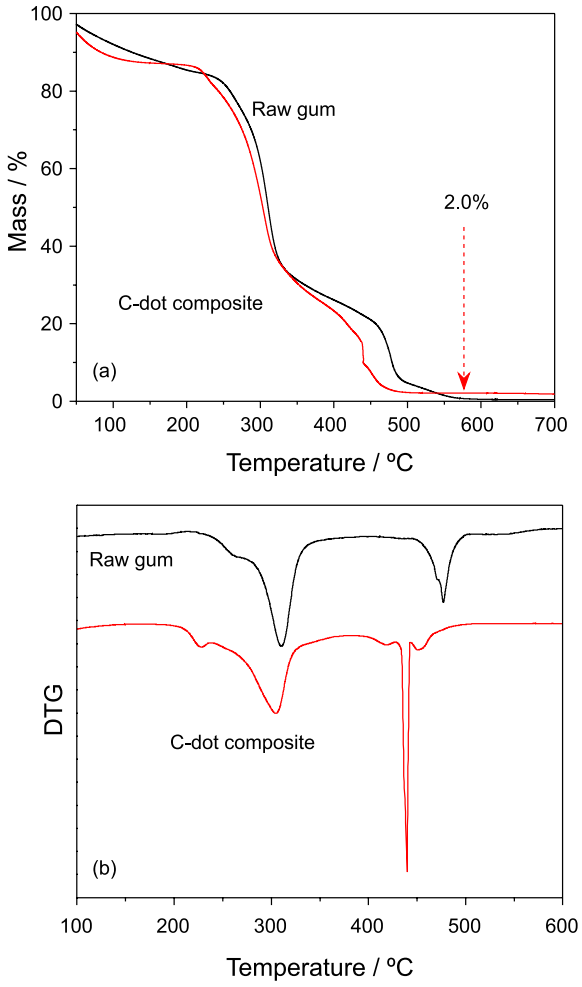

Figure 4. (a) TGA curves for raw cashew gum and C-dot composite in synthetic air; (b) differential thermogravimetry (DTG) curves related to TGA.

was insignificant. The presence of low carbon content in the core assumed in the GPC discussion was confirmed.

Proposed model for C-dots obtained from raw cashew gum

The synthetic procedure for the C-dot composite is depicted in Scheme 1a and the proposed model for the C-dot is shown in Scheme 1b. The carbon quantum dots obtained from raw cashew gum were not isolated from the composite, but the results indicated that they are comprised of a core of tiny carbon particles decorated with an oligosaccharide chain. The oligosaccharide shell functions as a self-passivation layer. The carbogenic particles represent around 10% (m/m) and the residual polysaccharide 90% (m/m).

Proposed mechanism for carbon dot formation

There are two main steps involved in this C-dot synthesis procedure: step 1, microwave heating of solution

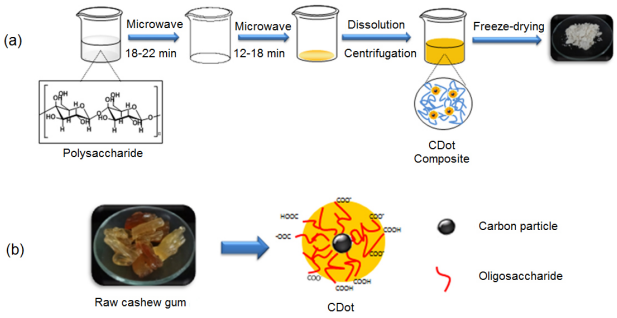

Scheme 1. (a) Schematic representation of the procedure used to obtain the C-dot composite from raw cashew gum; (b) proposed model for carbogenic C-dots.

for 18-22 min; and step 2, partial carbonization of the dried solution by microwave for 12-18 min.

The occurrence of partial depolymerization during the synthesis of the C-dots (steps 1 and 2) is suggested by the gel permeation chromatography results shown in Figure 3b. To investigate the possibility of depolymerization in the first step, the raw cashew gum solution was submitted to microwave irradiation under the conditions used in the C-dot preparation, but in this case the irradiation was continued until the total evaporation of water occurred (after 20 min), which characterized the end of step 1. Mpk was calculated based on equation 1. A decrease in the Mpk from an initial value of 30,400 to 22,000 g mol^{-1} was observed with 15 min of irradiation (Figure 5). This can be attributed to chain cleavage caused by the partial autohydrolysis of the polysaccharide.

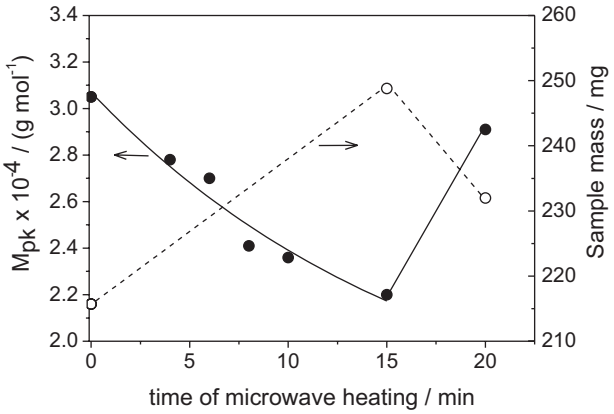

Figure 5. Effect of microwave irradiation time on the molar mass and residual mass of polysaccharide during the first step of carbon dot synthesis.

The microwave-assisted autohydrolysis of corn pericarp (cellulose, starch and arabinoxylan) was more efficient, with the production of monosaccharide units (arabinose, galactose, glucose, xylose and mannose), but at temperatures higher than 140 °C and with high pressure

systems.[30] Oligosaccharides,[30,31] and polyphenols[30] were also generated. The microwave-assisted hydrothermal depolymerization of cellulose at temperatures higher than 180 °C was reported and a very representative scheme was presented by the authors.[32] The decomposition of monosaccharides due to autohydrolysis with the production of 5-hydroxymethyl furfural (5-HMF) (from hexoses) and furfural (from pentoses) was observed at 200 °C with 30 min of microwave in high pressure systems.[33] Under the microwave-assisted experimental conditions (temperature less than 100 °C and atmosphere pressure) the partial autohydrolysis of raw cashew gum solution occurred.

The main monosaccharide units of cashew gum are hexoses: galactose (72-73 wt.%), glucose (11-14 wt.%), rhamnose (3.2-4 wt.%) and glucuronic acid (4.7-6.3 wt.%). The only pentose is arabinose which represents only 4.6-5 wt.% of the total sugar units.[22,24] A simple experiment was performed to analyze the possibility of depolymerization with the production of 5-HMF (from hexoses), and furfural (from pentoses).[29,33] The solutions were evaporated at low temperature to determine the mass of solid at different microwave irradiation times (0, 15 and 20 min). It was observed that the mass increased from the original solution to that irradiated for 15 min (Figure 5), the opposite trend to that observed for the Mpk.

During the autohydrolysis, a molecule of water is included in the reaction product at each chain cleavage. After 15 min of irradiation, the large increase in the mass (15.3%) compared with the small decrease in the Mpk (3.6%) suggests that monosaccharides or oligosaccharides of Mpk less than 1000 g mol^{-1} (column detection limit) were formed during the depolymerization. For example, if the bond breakage occurs in the middle of the chain, Mpk will be reduced to a half value with only one cleavage, and only one water molecule will be added *per* macromolecule. The decrease in the Mpk will be large and the increase in the mass will be small, which is in contrast to the results obtained.

After 20 min of irradiation there was an increase in the Mpk and decrease in the mass. The increase in the Mpk may be due to a low degree of crosslinking between the polysaccharide chains, as also reported by White *et al*.[34] for the pyrolysis of alginic acid. Considering the formation of monosaccharides due to autohydrolysis, the subsequent reaction, that is, the formation of 5-HMF, may explain the mass increase, because two water molecules are lost *per* each monosaccharide molecule. Due to the experimental conditions, which differ from those reported in the literature (higher temperature, pressure and time), the 5-HMF formation will be low. Scheme 2 shows the above-mentioned possible scenarios.

Step 2 can involve the formation of more 5-HMF and partial carbonization. 5-HMF molecules are absent during the pyrolysis of arabic gum (arabinogalactan, which is similar to cashew gum), probably because the C-6 atom of the hexose monosaccharide in the gum is involved in the glycosidic bond.[36] The formation of a hydrophobic carbon core within a hydrophilic shell has been reported for the hydrothermal carbonization of saccharides (glucose, sucrose and starch), but for microspheres and not nanospheres.[37]

The hydrophilic shell contains a high concentration of reactive oxygen groups (i.e., hydroxyl, phenolic, carbonyl, or carboxylic), some of them present in the C-dots obtained from cashew gum. The presence of partially depolymerized polysaccharide mixed with C-dots in the final product may be explained by the Scheme 3. The mass of cashew gum obtained after the water evaporation is around 200 mg. Large samples were associated with mass higher than 100 μg.[38] The solid deposited on the bottom of the beaker (end of step 1) forms a non-uniform layer with partially depolymerized polysaccharide, oligomers, and few monomers. During the step 2, the molecules close to the hot surface can absorb sufficient thermal energy and microwave irradiation to form carbonaceous material, with the volatilization of CO_2 and water. In other parts of the solid, less thermal energy and microwave irradiation leads to continue the depolymerization of polysaccharide.

Comparison of carbon dots obtained from natural precursors

The composite yield (17 ± 5% m/m) is in the range of those reported for C-dots obtained from other polysaccharides (7.8-34.6%),[9,10] and much higher than those produced from paper ash (0.05%)[26] (Table 1). The difference between the values obtained for peach gum and cashew gum may be due to the prior purification in the case of the former.[10] The quantum yield (8.7 ± 2) is comparable with those of C-dots obtained from some other raw materials, e.g., paper ash (9.3%)[26] and banana juice (8.9%),[35] and higher than others, e.g., bagasse (4.7%),[4] and plant peel extract (1.2%).[39] The Φ value for the C-dot composite is even higher than that reported for another polysaccharide (peach gum, 5.3%).[10] The zeta potential of an aqueous solution of the C-dot composite (–22.4 ± 1.1 mV) is higher than that of the raw gum (–2.9 ± 0.4 mV), indicating that negatively charged groups are present on the nanoparticle surface. This may be due to the formation of new carboxylate groups and/or greater exposure in the case of the negatively charged groups present in branched cashew gum (Pζ –9.8 ± 0.7 mV).[40]

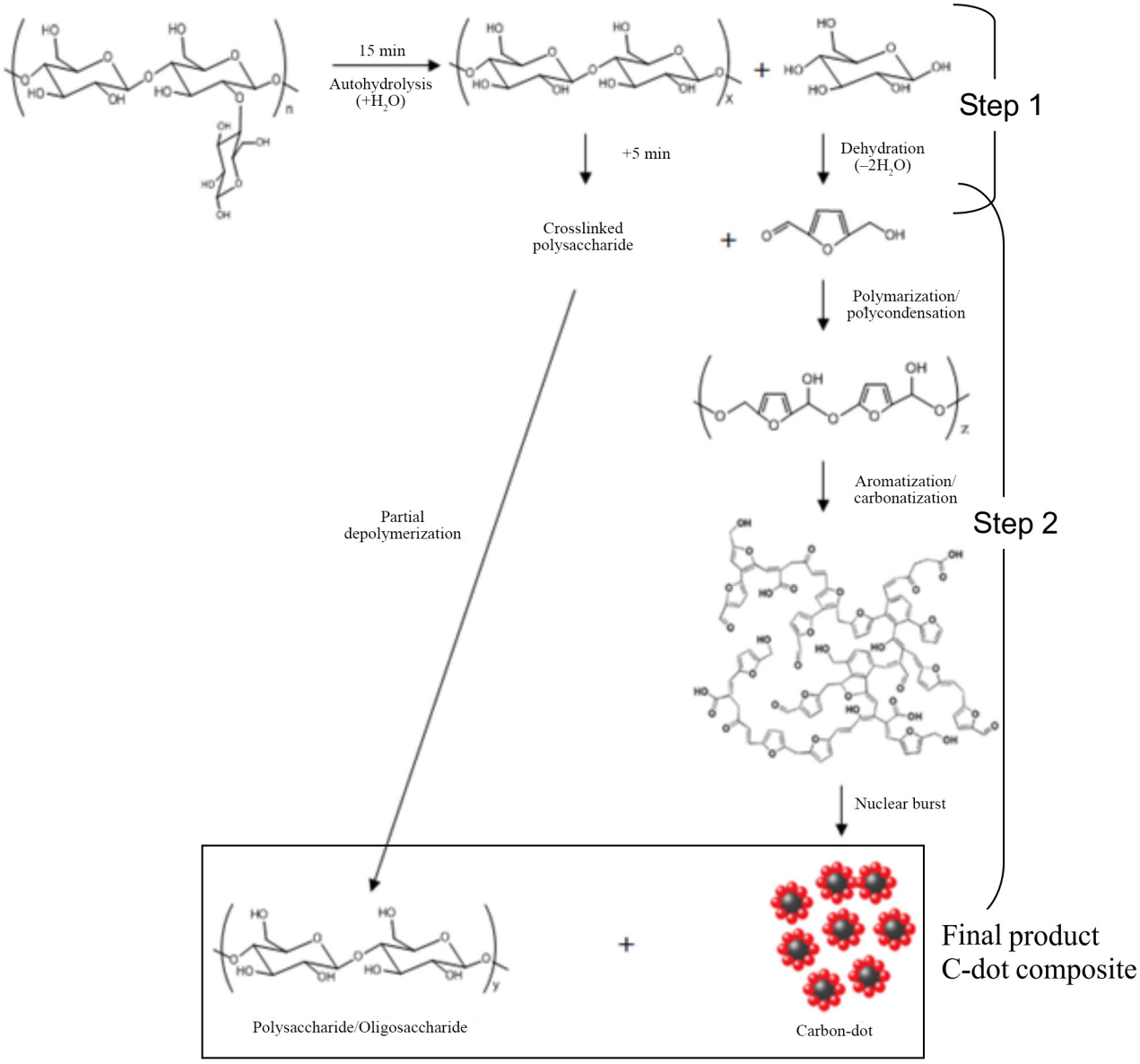

Scheme 2. Possible mechanism involved in the microwave-assisted two-step synthesis of carbon dots from raw cashew gum (adapted from De and Karak).[35] The polymerization degree (n, x, y) follows the order: n > x > y.

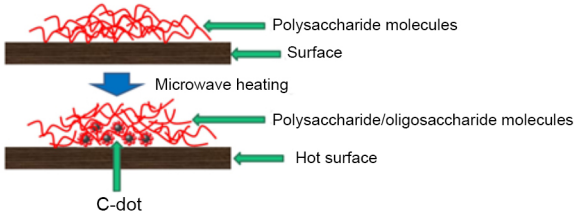

Scheme 3. Schematic representation of the production of the C-dot composite (adapted from Lomax, Boon and Hoffmann).[38]

Taking into account that the photoluminescent particle represents only 10% of the C-dot composite, and the oligosaccharide is not luminescent, the C-dots obtained from raw cashew gum must have a more intense optical emission, with a quantum yield much higher than 8.7%. The Φ value for isolated C-dots is not expected to reach values ten times higher than that observed for the composite, but instead in the order of 40%. Further studies are currently underway aimed at isolating the C-dots and increasing the percentage of carbogenic dots applying different experimental conditions.

Conclusions

The novel microwave-assisted synthesis of carbon quantum dots from raw polysaccharide material (cashew gum) involves 2 steps: partial depolymerization in solution and carbonization in a solid. The synthesis is easy, fast, cost effective and based on a totally green procedure. No

Table 1. Comparison of C-dots obtained from natural precursors

Precursor	Method	time consumed / h	Yield / wt.%	Φ value[a] / %	Diameter / nm	Pζ / mV	Ref.
Bagasse	alkalHT	58	NI	4.7	2.9	NI	4
Orange juice	HT	2.5	NI	26	2.5	–33.6	6
Gelatin	HT	3	38.6	31.6	1.7	NI	7
Sugar cane juice	HT	3	NI	5.8	3.0	NI	8
Chitosan	HT	12	7.8	NI	5	NI	9
Peach gum	HT	12	34.6	5.3	2-5	NI	10
Glycerol	MW	0.23	NI	3.2	2.1	NI	18
Plant leaf	PY N_2	2	NI	11.8-16.4	3.7	NI	21
Paper ash	PY	NI	0.05	9.3	3	–10.6	26
Plant peel extract	HT	2	NI	1.2	7	NI	39
Cashew gum	MW	0.7	17.5	8.7	9	–22.4	This work

[a]Quinine sulfate as standard. HT: hydrothermal treatment; MW: microwave heating; PY: pyrolysis; NI: not informed by authors.

external passivation or functionalization was applied and a photoluminescent nanoparticle with a good quantum yield was obtained. A mechanism for the two steps was suggested based on experiments and results reported in the literature. The expected no toxicity and negative charge on C-dot surface improves hydrophilicity and stability in aqueous system, and indicates the possibility of use in *in vivo* imaging.

Acknowledgements

This study was supported by the National Institute for Science and Technology (INCT-INOMAT), and CNPq. Special acknowledgments are due to Prof F. Galembeck and Douglas S. da Silva for the EFTEM facilities.

References

1. Xu, X. Y.; Ray, R.; Gu, Y. L.; Ploehn, H. J.; Gearheart, L.; Raker, K.; Scrivens, W. A.; *J. Am. Chem. Soc*. **2004**, *126*, 12736.
2. Esteves da Silva, J. C. G.; Gonçalves, H. M. R.; *TrAC - Trends Anal. Chem*. **2011**, *30*, 1327.
3. Li, H.; Zhang, Z.; Liu, Y.; Lee, S.-T.; *J. Mater. Chem*. **2012**, *22*, 24230.
4. Liu, X.-J.; Guo, M.-L.; Huang, J.; Yin, X.-Y.; *Bioresources* **2013**, *8*, 2537.
5. Huang, H.; Xu, Y.; Tang, C.-J.; Chen, J.-R.; Wang, A.-J.; Feng, J.-J.; *New J. Chem.* **2014**, *38*, 784.
6. Sahu, S.; Behera, B.; Maiti, T. K.; Mohapatra, S.; *Chem. Commun*. **2012**, *48*, 8835.
7. Liang, Q.; Ma, W.; Shi, Y.; Li, Z.; Yang, X.; *Carbon* **2013**, *60*, 421.
8. Mehta, V. N.; Jha, S.; Kailasa, S. K.; *Mater. Sci. Eng., C* **2014**, *38*, 20.
9. Yang, Y.; Cui, J.; Zheng, M.; Hu, C.; Tan, S.; Xiao, Y.; Yang, Q.; Liu, Y.; *Chem. Commun*. **2012**, *48*, 380.
10. Zhou, L.; He, B.; Huang, J.; *Chem. Commun*. **2013**, *49*, 8078.
11. Liu, S.; Tian, J.; Wang, L.; Luo, Y.; Sun, X.; *RSC Adv.* **2012**, *2*, 411.
12. Zhai, X.; Zhang, P.; Liu, C.; Bai, T.; Li, W.; Dai, L.; Liu, W.; *Chem. Commun*. **2012**, *48*, 7955.
13. Hou, J.; Yan, J.; Zhao, Q.; Li, Y.; Ding, H.; Ding, L.; *Nanoscale* **2013**, *5*, 9558.
14. Dey, S.; Chithaiah, P.; Belawadi, S.; Biswas, K.; Rao, C. N. R.; *J. Mater. Res.* **2014**, *29*, 383.
15. Tang, Y.; Su, Y.; Yang, N.; Zhang, L.; Lv, Y.; *Anal. Chem.* **2014**, *86*, 4528.
16. Chandra, S.; Pathan, S. H.; Mitra, S.; Modha, B. H.; Goswami, A.; Pramanik, P.; *RSC Adv.* **2012**, *2*, 3602.
17. Zhao, L.; Di, F.; Wang, D.; Guo, L.-H.; Yang, Y.; Wan, B.; Zhang, H.; *Nanoscale* **2013**, *5*, 2655.
18. Wang, X.; Qu, K.; Xu, B.; Ren, J.; Qu, X.; *J. Mater. Chem*. **2011**, *21*, 2445.
19. Peng, H.; Travas-Sejdic, J.; *Chem. Mater*. **2009**, *21*, 5563.
20. Li, Y.; Zhong, X.; Rider, A. E.; Furman, S. A.; Ostrikov, K.; *Green Chem.* **2014**, *16*, 2566.
21. Zhu, L.; Yin, Y.; Wang, C.-F.; Chen, S.; *J. Mater. Chem. C* **2013**, *1*, 4925.
22. de Paula, R. C. M.; Rodrigues, J. F.; *Carbohydr. Polym.* **1995**, *26*, 177.
23. Costa, S. M. O.; Rodrigues, J. F.; de Paula, R. C. M.; *Polim.: Cienc. Tecnol.* **1996**, *abr/jun*, 49.
24. Cunha, P. L. R.; de Paula, R. C. M.; Feitosa, J. P. A.; *Quim. Nova* **2009**, *32*, 649.
25. Sun, Y.-P.; Zhou, B.; Lin, Y.; Wang, W.; Shiral Fernando, K. A.; Pathak, P.; Meziani, M. J.; Harruff, B. A.; Wang, X.; Wang, H.; Luo, P. G.; Yang, H.; Kose, M. E.; Chen, B.; Veca, L. M.; Xie, S.-Y.; *J. Am. Chem. Soc.* **2006**, *128*, 7756.
26. Wei, J.; Shen, J.; Zhang, X.; Guo, S.; Pan, J.; Hou, X.; Zhang, H.; Wang, L.; Feng, B.; *RSC Adv.* **2013**, *3*, 13119.
27. Zhang, J.; Shen, W.; Pan, D.; Zhang, Z.; Fang, Y.; Wu, M.; *New J. Chem*. **2010**, *34*, 591.

28. Mothé, C. G.; Freitas, J. S.; *J. Therm. Anal. Calorim.* **2014**, *116*, 1509.
29. Jiang, W.; Nadeau, G.; Zaghib, K.; Kinoshita, K.; *Thermochim. Acta* **2000**, *351*, 85.
30. Yoshida, T.; Tsubaki, S.; Teramoto, Y.; Azuma, J.; *Bioresour. Technol.* **2010**, *101*, 7820.
31. Matsumoto, A.; Tsubaki, S.; Sakamoto, M.; Azuma, J.; *Bioresour. Technol.* **2011**, *102*, 3985.
32. Fan, J.; De Bruyn, M.; Budarin, V. L.; Gronnow, M. J.; Shuttleworth, P. S.; Brenden, S.; Macquarrie, D. J.; Clark, J. H.; *J. Am. Chem. Soc*. **2013**, *135*, 11728.
33. Tsubaki, S.; Oono, K.; Onda, A.; Yanagisawa, K.; Azuma, J.; *Carbohydr. Res*. **2013**, *375*, 1.
34. White, R. J.; Antonio, C.; Budarin, V. L.; Bergstrom, E.; Thomas-Oates, J.; Clark, J. H.; *Adv. Funct. Mater.* **2010**, *20*, 1834.
35. De, B.; Karak, N.; *RSC Adv.* **2013**, *3*, 8286.
36. Chiantore, O.; Riedo, C.; Scalarone, D.; *Int. J. Mass Spectrom*. **2009**, *284*, 35.
37. Sevilla, M.; Fuertes, A. B.; *Chem. Eur. J.* **2009**, *15*, 4195.
38. Lomax, J. A.; Boon, J. J.; Hoffmann, R. A.; *Carbohydr. Res*. **1991**, *221*, 219.
39. Mewada, A.; Pandey, S.; Shinde, S.; Mishra, N.; Oza, G.; Thakur, M.; Sharon, M.; Sharon, M.; *Mater. Sci Eng., C* **2013**, *33*, 2914.
40. Cunha, P. L. R.; Maciel, J. S.; Sierakowski, M. R.; de Paula, R. C. M.; Feitosa, J. P. A.; *J. Braz. Chem. Soc.* **2007**, *18*, 85.

Submitted: December 16, 2014
Published online: April 24, 2015